

Published in final edited form as:

*Mult Scler.* 2000 June ; 6(3): 148–155.

## **<sup>1</sup>H MRSI comparison of white matter and lesions in primary progressive and relapsing-remitting MS**

**J Suhy<sup>\*,1,3</sup>, WD Rooney<sup>1,3,4</sup>, DE Goodkin<sup>2</sup>, AA Capizzano<sup>1,3</sup>, BJ Soher<sup>1,3</sup>, AA Maudsley<sup>1,3</sup>, E Waubant<sup>2</sup>, PB Andersson<sup>2</sup>, and MW Weiner<sup>1,3</sup>**

<sup>1</sup>Department of Radiology, University of California at San Francisco, San Francisco, California, USA

<sup>2</sup>Department of Neurology, University of California at San Francisco, San Francisco, California, USA

<sup>3</sup>Magnetic Resonance Unit, DVA Medical Center, San Francisco, California, CA 94121, USA

<sup>4</sup>Chemistry Department, Brookhaven National Laboratory, Upton, New York, NY 11973, USA

### **Abstract**

**Objective**—To compare brain metabolite levels in patients with primary progressive (PP) and relapsing remitting (RR) MS and controls. Hypotheses: (1) creatine (Cr), a putative marker of gliosis, is elevated and N-acetylaspartate (NAA), a putative marker of axonal density and functional integrity, is reduced in PPMS lesions and normal appearing white matter (NAWM) compared to control white matter; (2) The pattern of metabolite change in PPMS is different than in RRMS.

**Methods**—MRI and proton magnetic resonance spectroscopic imaging (<sup>1</sup>H MRSI) were collected from 15 PPMS patients, 13 RRMS patients, and 20 controls.

**Results**—Cr was increased in PPMS NAWM compared to controls (P=0.035), and compared to RRMS NAWM (P=0.038). Cr was increased in focal MRI lesions from PPMS compared to lesions from RRMS (P=0.044) and compared to control white matter (P=0.041). NAA was similarly reduced in PPMS and RRMS NAWM compared to control. NAA was similarly reduced in PPMS and RRMS lesions, compared to control white matter.

**Conclusions**—Creatine is higher in PPMS than RRMS NAWM and focal lesions. This observation is consistent with the notion that progressive disability in PPMS reflects increased gliosis and axonal loss whereas disability in RRMS reflects the cumulative effects of acute inflammatory lesions and axonal loss.

### **Keywords**

*primary progressive multiple sclerosis; magnetic resonance spectroscopy*

### **Introduction**

Multiple Sclerosis (MS) is an inflammatory demyelinating disease of the central nervous system with distinct clinical subtypes. Approximately 85% of patients initially experience acute onset of symptoms that generally remit spontaneously; this disease subtype is termed relapsing-remitting MS (RRMS). Approximately 50% of RRMS patients eventually experience gradual progression of disability that may or may not be accompanied by acute

relapses; this disease subtype is termed secondary progressive MS (SPMS). Approximately 15% of MS patients experience a clinical pattern that is progressive from onset; a subtype termed primary progressive MS<sup>1</sup> (PPMS). The pathological hallmark of all subtypes of MS are focal lesions that are distinguished by their content of activated macrophages and T cells, edema, demyelination, and axonal transection.<sup>2</sup> Each of these histopathologies<sup>3</sup> appears hyperintense on T2-weighted MRI. The white matter, which appears normal on gross pathology, shows mostly astroglial hypertrophy and to a much lesser extent inflammatory infiltrate, demyelination or axonal loss.<sup>4</sup>

Multiple lines of evidence suggest that the biology of PPMS differs significantly from that of RRMS and SPMS. Cross-sectional and longitudinal MRI studies indicate that compared to RRMS and SPMS, PPMS patients are more likely to experience: (1) fewer focal intracranial and spinal gadolinium-enhancing and T2-weighted MRI lesions;<sup>5-8</sup> (2) more diffuse abnormalities in the white matter of the spinal cord;<sup>9</sup> and (3) more progressive atrophy of the spinal cord as measured by cross sectional diameter at C2 - 3.<sup>10</sup> Immunological markers of disease activity indicate serum levels of soluble E-selectin are increased in patients with PPMS<sup>11</sup> and cerebrospinal fluid (CSF) levels of sE-selectin are significantly raised in PPMS compared to RRMS during relapse and remission.<sup>12</sup> PPMS may be genetically distinct from RR and SPMS.<sup>13-15</sup> The extent of inflammatory perivascular infiltrates in lesions is less severe in PPMS than RRMS and SPMS.<sup>16</sup> The possibility that diffuse imaging abnormalities in white matter of PPMS largely reflect increased gliosis rather than or in addition to axonal loss has never been explicitly considered. Further, there has never been a rigorous study comparing the histopathology of normal appearing white matter in PPMS, and RRMS.

Although magnetic resonance spectroscopy (MRS) and magnetic resonance spectroscopic imaging (MRSI) may improve the histopathological specificity of T2-weighted MR imaging changes observed in MS,<sup>5,6</sup> there have been few MRS and MRSI studies comparing lesions and normal appearing white matter (NAWM) in PPMS, and RRMS. Most MRS and MRSI studies of patients with MS have measured the following metabolites: N-acetyl aspartate (NAA), which has been suggested to be a marker for neuron viability and axonal density in the brain,<sup>17</sup> Creatine (Cr) which represents a combination of creatine and phosphocreatine, a putative marker of gliosis,<sup>18,19</sup> and Choline (Cho) thought to be a marker associated with membrane phospholipids.<sup>20</sup> <sup>1</sup>H MRS studies of RRMS show reduced NAA/Cr in T2-intense lesions<sup>21</sup> and normal appearing white matter.<sup>22-24</sup> Presumably, these metabolic changes in normal appearing white matter reflect microscopic disease<sup>4</sup> and decreased NAA/Cr in lesions and normal appearing white matter of RRMS probably reflects decreased NAA and increased Cr.<sup>21,25,26</sup> NAA is shown to be similarly reduced in MRI lesions of PPMS and RRMS<sup>27</sup> and NAA is also decreased in normal appearing white matter in PPMS<sup>28,29</sup> compared to white matter in controls. Nonetheless, a rigorous comparison of NAA and Cr in both lesions and normal appearing white matter in PPMS, RRMS and white matter in controls has never been reported. Previous studies have reported that Cr is increased in RRMS normal appearing white matter compared to white matter of healthy controls. The increased Cr has been attributed to microscopic disease, most likely gliosis. Since PPMS is considered to have much less inflammatory disease than RRMS, comparison of Cr levels between RRMS and PPMS could be instructive. If NAA is similarly reduced in PPMS and RRMS normal appearing white matter, an increase in Cr in PPMS normal appearing white matter and focal lesions relative to RRMS would be consistent with the notion that sustained progression of disability in PPMS reflects gliosis in addition to inflammation and axonal loss.

The goal of this study was to compare levels of Cr and NAA in lesions and normal appearing white matter in PPMS, RRMS and white matter in controls. The specific *a priori* hypotheses tested were, that compared to control white matter: (1) Cr is increased in PPMS normal appearing white matter and lesions reflecting a possible increase in diffuse gliosis and (2) NAA

is decreased in PPMS normal appearing white matter and lesions. A secondary objective was to determine whether the pattern of metabolite change was different in RRMS and PPMS and reflected known differences in the histopathology of RRMS and PPMS.

## Materials and methods

### Subjects

This study was approved by the Committee on Human Research at the University of California, San Francisco, and all subjects provided written informed consent prior to MRI and MRS examination. Patients with clinically definite MS<sup>30</sup> who met consensus criteria<sup>1,31,32</sup> for different clinical disease patterns were enrolled. Fifteen patients with PPMS (ten males and five females; mean age, 47.5 years; mean EDSS score, 4.40; mean disease duration, 9.07 years), 13 patients with RRMS (seven males and six females; mean age, 39.5 years; mean EDSS score, 2.50; mean disease duration 7.79 years), and 20 healthy controls (13 males and seven females; age range 24 - 59 years; mean age, 41.3 years) were investigated by MRI and long-TE PRESS <sup>1</sup>H MRSI. The lesions of 12 PPMS (5.17±5.2 lesions per MRSI volume of interest) and ten RRMS (3.10±2.5 lesions per MRSI volume of interest) patients were studied, since only these patients had lesions present in the VOI. The subjects with RRMS have been previously studied by MRI/<sup>1</sup>H MRSI and the results have been reported.<sup>26</sup> Therefore, no *a priori* hypotheses were tested concerning the RRMS subjects. However, to allow comparison with PPMS, the data from the RRMS subjects was reanalyzed by the identical methods used to analyze the PPMS. The RRMS data was re-fitted with updated automated software and voxel selections were redone to be consistent with how voxels were selected for the PPMS data.

### Magnetic resonance imaging

All MR data were acquired on a 1.5 Tesla Magnetom VISION system (Siemens Inc., Germany) equipped with a standard quadrature head coil. Proton density and T2-weighted MRI images were acquired using a double spin echo sequence (TE 20/80 ms, TR 2500 ms, 3 mm slice thickness) angulated parallel to the anterior commissure-posterior commissure (AC-PC) line. Fifty-one axial slices, without gap, were acquired with a 192×256 matrix over a 180×240 mm field of view (FOV).

### Magnetic resonance spectroscopic imaging

Water suppressed 2D <sup>1</sup>H MRSI data sets were acquired using a PRESS spin-echo sequence (TE 135 msec, TR 1800 ms). <sup>1</sup>H MRSI data were acquired from two volumes of interest (VOI); the first in the centrum semiovale centered above the corpus callosum and the second was centered on the lateral ventricles as seen in the sagittal scout images. Each of these brick-shaped VOI's was angulated parallel to the AC-PC line and adjusted for each patient to maximize white matter signal while avoiding lipid in the skull and scalp. The <sup>1</sup>H MRSI FOV was 210×210 mm and was obtained using a circular *k*-space acquisition scheme<sup>33</sup> that encoded 24 steps along each of the major axes. The total number of phase encoding permutations was 448. Since one signal average was collected at each phase encoding step, the total acquisition time was 13 min. The spectroscopy data was apodized in the spatial frequency domain using a Gaussian filter that produced an effective voxel size of 2.4 cm<sup>3</sup>. A non-uniform spectral intensity profile across the left-right VOI, due to a non-optimized slice-selective refocusing pulse of the PRESS sequence, was corrected using an empirical correction function.

### Voxel selection

A neuroradiologist identified MS lesion and normal appearing white matter regions on T2-weighted MRI. Figure 1A shows the area over which spectroscopic imaging was performed by the rectangles on the midsagittal image. Normal appearing white matter voxels were selected

from the centrum semiovale VOI (Figure 1B) and lesion voxels were selected from the periventricular VOI (Figure 1C). The white circles in the figures represent the voxels that were selected. A representative  $^1\text{H}$  MRSI spectrum is shown in Figure 1D with the Cho, Cr, and NAA resonances labeled. Spectroscopic imaging data were displayed and voxels were selected using a software program that was developed in house.<sup>34</sup> Corresponding periventricular white matter (PVWM)  $^1\text{H}$  MRSI voxels were selected from the controls for a spatially analogous (z position) comparison to MS lesion. The maximum number of normal appearing white matter voxels was selected that did not include MS lesions, gray matter, or CSF (through all five 3 mm MRI slices of each PRESS box, plus one slice above and below the PRESS box). Within the  $^1\text{H}$  MRSI imaging plane, selected normal appearing white matter voxels were at least one voxel away from lesions, gray matter, and CSF regions. For the MS lesion, voxels were selected and grouped according to the number of MRI slices in the VOI that each lesion encompassed (one to five slices). Only lesions that were present in at least 60% (three or more MRI slices) of the VOI were averaged. Voxels of the controls were selected from brain regions that were spatially analogous to those of the patients. Voxels between MS patient groups were matched as best as allowed by variances in lesion location and number.

### Spectral analysis

$^1\text{H}$  MRSI data were zero-filled to a matrix of  $32 \times 32 \times 1024$  points and Fourier transformed. Spectra were fitted using an automated curve-fitting program that was developed in-house<sup>35</sup> using a Lorentzian-Gaussian lineshape model for the three singlet peaks of Cho, Cr, and NAA. CSF water was used as the standard to normalize the spectroscopy data.<sup>36</sup> Integrated intensities of the three singlet peaks were corrected for coil loading, receiver gain, and normalized to the mean proton density MRI intensity of four CSF regions of interest (ROI). The CSF ROI's were positioned entirely within the lateral ventricles of a proton density image that was acquired during the same session as the spectroscopy data. To avoid contribution from the choroid plexus, the least contaminated CSF ROI's were selected as defined by having the greatest intensities on the proton density image. The equation used to normalize the spectroscopy data was:

$$\text{Met}_{\text{norm}} = (\text{Met}_{\text{raw}} / \text{CSF}_{\text{raw}}) (TV_{\text{MRSI}} / TV_{\text{MRI}}) (\text{fft}_{\text{MRI}}) 10 (\text{gain}_{\text{MRI}} - \text{gain}_{\text{MRSI}}) / 20 \quad (1)$$

where  $\text{Met}_{\text{norm}}$  is the normalized metabolite value,  $\text{Met}_{\text{raw}}$  is the raw metabolite value,  $\text{CSF}_{\text{raw}}$  is the intensity of the CSF on the proton density,  $TV_{\text{MRSI}}$  and  $TV_{\text{MRI}}$  are the transmitter reference voltages of the MRSI and MRI, respectively,  $\text{fft}_{\text{MRI}}$  is the fft scaling factor of the MRI, and  $\text{gain}_{\text{MRI}}$  and  $\text{gain}_{\text{MRSI}}$  are the receiver gains of the MRI and MRSI, respectively. The  $\text{fft}_{\text{MRSI}}$  does not appear in the equation because it was the same for all  $^1\text{H}$  MRSI studies.

### Statistical analysis

MRI and  $^1\text{H}$  MRSI acquisitions were performed by two different operators, but a single operator performed all data processing. After all the data were acquired and processed, statistical analyses were performed to determine if there was any effect of operator on the data. The results showed some operator dependence for Cho and not for any other metabolites, likely due to systematic differences in the adjustment of water suppression pulses between operators. Since there were no significant between group differences for Cho, this operator dependence has no effect on the data analysis or interpretation.

Values are reported as mean  $\pm$  standard deviation (s.d.). Analysis of variance (ANOVA) was used to assess differences between the control and patient groups. A Benjamini-Hochberg adjustment<sup>37</sup> was used to correct for multiple comparisons as applicable according to the *a priori* hypotheses of increased Cr and decreased NAA in PPMS. The level of significance was

$P < 0.05$ . Since there were age, EDSS score, disease duration, and number of lesions in the VOI differences between groups, we determined if these variables had any effects on the measures of interest by analysis of covariance (ANCOVA) and regression analysis. An age-dependence was found only for Cr within the control group white matter (Figure 2A) and was corrected using a linear model. All comparisons between the control and patient groups were performed using age-corrected control data. The patient groups did not have an age-dependence for Cr (Figure 2B).

## Results

### Normal appearing white matter

Mean group values of NAA/Cr, and NAA/Cho measures from normal appearing white matter regions are summarized in Table 1. NAA/Cr of PPMS ( $1.90 \pm 0.11$ ) was significantly decreased compared to RRMS ( $2.04 \pm 0.09$ ,  $P = 0.031$ ) and to controls ( $2.22 \pm 0.19$ ,  $P = 0.027$ ). NAA/Cr in RRMS was also significantly decreased compared to controls ( $P = 0.027$ ), similar to our previous report.<sup>26</sup> NAA/Cr of PPMS, but not RRMS, was significantly related to EDSS score ( $P = 0.025$ ,  $r^2 = 0.67$ ). No significant between group NAA/Cho differences were found.

To determine if decreased NAA/Cr in normal appearing white matter was due to change of NAA or Cr, CSF normalized metabolite values were calculated and are shown in Table 1. Cr was significantly higher in RRMS than controls ( $P = 0.044$ ). This result is consistent with earlier observations.<sup>26</sup> Cr was also increased in PPMS when compared to controls ( $P = 0.035$ ) and RRMS ( $P = 0.038$ ). The differences between patients and controls were not attributable to an interaction between Cr and age and the differences between PPMS and RRMS were not attributable to any interaction between Cr and age, EDSS score, disease duration, or number of lesions in the VOI.

Although NAA in PPMS and RRMS were similar, NAA was lower in normal appearing white matter of PPMS and RRMS than controls ( $P = 0.047$  and  $P = 0.047$ ). Thus decreased NAA/Cr in PPMS compared to RRMS reflected an increase in Cr in normal appearing white matter of PPMS. In contrast, decreased NAA/Cr in PPMS and RRMS compared to controls reflected increased Cr and decreased NAA. Unlike our results for the NAA/Cr ratio, EDSS score was not correlated with NAA and Cr separately.

### Focal T2-hyperintense lesions

NAA/Cr was significantly reduced in lesions in PPMS and RRMS compared to white matter of controls ( $P = 0.027$  and  $P = 0.048$ ). NAA/Cr was similar in PPMS and RRMS and NAA/Cho was similar in PPMS, RRMS, and controls. In contrast to NAA/Cr in normal appearing white matter, NAA/Cr in focal lesions in PPMS and RRMS was not related to EDSS score.

In order to determine whether decreased NAA/Cr in focal lesions was due to change of NAA or Cr, CSF normalized metabolite values were calculated and are summarized in Table 2. Cr in focal lesions in PPMS was significantly increased when compared to RRMS lesions and control white matter ( $P = 0.044$  and  $P = 0.041$ ). In contrast, Cr in RRMS lesions was similar to Cr in control white matter. NAA in PPMS and RRMS lesions was significantly lower than control NAA ( $P = 0.036$  and  $P = 0.031$ ). In contrast, NAA in PPMS and RRMS lesions were similar. Thus, decreased NAA/Cr in PPMS compared to controls reflected increased Cr and decreased NAA.

## Discussion

Our observations indicate: (1) Cr is increased, and NAA decreased in PPMS normal appearing white matter and lesions compared to control white matter; (2) Cr is increased in both normal

appearing white matter and lesions of PPMS compared to RRMS; and (3) NAA is similarly decreased in PPMS and RRMS normal appearing white matter and lesions compared to control white matter. These changes were independent of age, degree of disability by EDSS score, differences of disease duration, and number of lesions in VOI. Our results are in accordance with the report by Davie *et al.*,<sup>27</sup> that NAA is similarly reduced in focal lesions of patients with PPMS and RRMS. These results suggest that the extent of axonal dysfunction or axonal density, as measured by NAA, is similar in our sample of PPMS and RRMS.

To the best of our knowledge, this is the first report that Cr is increased in focal lesions and normal appearing white matter of patients with PPMS compared to patients with RRMS. The differences between patients and controls are independent of age and the differences between patients with PPMS and RRMS are independent of differences in age, EDSS score, disease duration, and number of lesions in the VOI.

Converging lines of evidence from natural history,<sup>32,38</sup> histopathology,<sup>2,3</sup> immunology,<sup>13-15</sup> and magnetic resonance imaging<sup>5-8</sup> studies suggest that the biology of PPMS differs significantly from that of RRMS and SPMS. However, fresh brain tissue from these patients is difficult to obtain, and as a result, rigorous histopathological studies to quantify and compare the extent of demyelination, axonal loss and gliosis in lesions and normal appearing white matter in PPMS and RRMS are lacking.

There is a notion that <sup>1</sup>H MRSI and magnetization transfer ratio (MTR) may provide surrogate markers of irreversible tissue damage in MS. <sup>1</sup>H MRS and <sup>1</sup>H MRSI provide quantitative measures of brain metabolites that have more histopathological specificity than conventional T2-weighted imaging. For example, measures of NAA, a putative marker of neuronal functional integrity and density, and the ratio NAA/Cr correlate more robustly with level of neurologic impairment and disability than measures of T2-weighted lesion load.<sup>39</sup> That NAA/Cr is reduced in lesions<sup>21</sup> and normal appearing white matter<sup>22,23</sup> in RRMS when compared to controls suggests that focal and diffuse axonal loss contribute to disability in these patients. However, NAA/Cr may also reflect changes in Cr, a putative marker of gliosis.<sup>18,19</sup>

The possibility that gliosis is a significant contributor to disability has never been explicitly considered in reports of <sup>1</sup>H MRSI in patients with MS. The <sup>1</sup>H MRS Cr signal intensity is much more variable than originally believed. It differs in normals between white and gray matter, it is increased in gray matter in aging,<sup>18</sup> and increases in some disease pathologies.<sup>21,25,26</sup> In this study we have observed an increase in white matter <sup>1</sup>H MRS Cr signal intensity with age in healthy controls. That we do not observe an increase in Cr with age in MS patients is likely the result that disease related increases in Cr signal intensity confound an age-related relationship in our small cohort of patients. The variability of the <sup>1</sup>H MRS Cr signal stresses the importance of absolute quantitation to improve the ability to interpret <sup>1</sup>H MRS data. Our observations show that: (1) NAA is similarly reduced in PPMS and RRMS normal appearing white matter; and (2) Cr is significantly increased in PPMS normal appearing white matter and lesions when compared to RRMS. These are consistent with the notion that sustained progression of disability in PPMS reflects diffuse gliosis and axonal loss, in contrast to RRMS where sustained progression of disability reflects diffuse axonal loss and multifocal inflammation.

We have considered the possibility that increased Cr observed in our patients with PPMS may reflect factors other than clinical subtype. First, our patient sample was small and may not be representative of the larger population of patients with PPMS and RRMS. We think this is unlikely because the clinical characteristics of our patients are typical of those reported by others.<sup>32,38</sup> Second, lower Cr in RRMS compared to PPMS might reflect dilution resulting from more pronounced microscopic inflammation and edema. We think this is unlikely because

NAA was similar in patients with PPMS and RRMS. Third, Cr increased with age in the control group. Thus, since the age at onset of disease is on average older for patients with PPMS than RRMS, it is possible that differences in age explain cross-sectional differences in Cr. We think this is unlikely because differences in Cr between patient groups persisted after controlling for differences in age and disease duration. Fourth, the PPMS group had on average a larger fraction of focal lesional white matter within the selected VOIs. Thus, since there is a negative correlation between NAA/Cr and distance from focal lesions,<sup>21</sup> it is possible that higher Cr in PPMS could be due to the greater number of visible focal lesions in that group. We think this is unlikely because we specifically selected normal appearing white matter voxels that were most distant from visible focal MS lesions, and also showed by ANCOVA that the metabolite differences were not dependent on the number of lesions in the VOI. The choice to study only large lesions, those present in at least 60% of the VOI, may have biased the results. However, large lesions needed to be used in order to minimize partial voluming effects. The results may be limited by the use of one-sided tests of significance and multiple comparison corrections.

We have also considered technical limitations that might influence the results of our study. First, the coarse spatial resolution of MRSI raises the possibility that data from lesions or normal appearing white matter was 'contaminated' by volume averaging from adjacent gray matter, CSF, or nearby focal lesions. Although voxels were carefully selected to include predominantly white matter for the normal appearing white matter data and lesion for the lesion data, contributions from other tissue types or partial-volume effects cannot be avoided due to the coarse spatial resolution of MRSI. In order to reduce spatially dependent sampling bias between groups, voxels were carefully selected to have virtually identical spatial distributions in all three groups. Also, an automated fitting program was used to eliminate operator bias and increase the number of voxels observed. Second, since signal intensities were not corrected for relaxation differences, metabolite changes observed may be due to altered relaxation properties. Finally, the equation used to normalize the spectroscopy data assumes identical T1 and T2 of CSF water and similar partial volume effects between subject groups.

In summary, our data confirm and extend previous reports that NAA in PPMS and RRMS normal appearing white matter and focal lesions is reduced when compared to controls. These observations are consistent with the notion that sustained progression of disability in MS is in part attributable to axonal loss.<sup>40</sup> That creatine is significantly more increased in PPMS than RRMS normal appearing white matter and focal lesions is consistent with the notion that sustained progression of disability in PPMS reflects diffuse gliosis and axonal loss. In contrast, sustained progression of disability in RRMS reflects diffuse axonal loss and multifocal inflammation. Quantitative histopathological examinations of normal appearing white matter and focal lesions in patients with PPMS and RRMS will be necessary to test this hypothesis.

## Acknowledgements

This study was supported in part by a grant in aid (MW Weiner), Grant RG 2655-A-4 (DE Goodkin), and a postdoctoral fellowship (J Suhy) all from the National Multiple Sclerosis Society, and PHS grant AG12119 (AA Maudsley).

## References

1. Thompson AJ, et al. Primary Progressive multiple sclerosis. *Brain* 1997;120:1085–1096. [PubMed: 9217691]
2. Raine C, Dale E, McFarlin Memorial Lecture: the immunology of the multiple sclerosis lesion. *Ann Neurol* 1994;36:S61–S72. [PubMed: 8017891]
3. Trapp B, et al. Axonal transection in the lesions of multiple sclerosis. *New Engl J Med* 1998;338:278–285. [PubMed: 9445407]
4. Allen IV, McKeown SR. A histological, histo-chemical and biochemical study of the macroscopically normal white matter in multiple sclerosis. *J Neurol Sci* 1979;41:81–91. [PubMed: 438845]

5. Silver NC, et al. Sensitivity of contrast enhanced MRI in multiple sclerosis; Effects of gadolinium dose, magnetization transfer contrast and delayed imaging. *Brain* 1997;120:1149–1161. [PubMed: 9236628]
6. Kidd D, et al. The transverse magnetization decay characteristics of longstanding lesions and normal-appearing white matter in multiple sclerosis. *J Neurol* 1997;244:125–130. [PubMed: 9120495]
7. Thompson AJ, et al. Major differences in the dynamics of primary and secondary progressive multiple sclerosis. *Ann Neurol* 1991;29:53–62. [PubMed: 1996879]
8. Filippi M, et al. Comparison of triple dose versus standard dose gadolinium-DTPA for detection of MRI enhancing lesions in patients with primary progressive multiple sclerosis. *J Neurol Neurosurg Psychiatry* 1995;59:540–544. [PubMed: 8530944]
9. Lycklama a Nijeholt GJ, et al. Brain and spinal cord abnormalities in multiple sclerosis: Correlation between MRI parameters, clinical subtypes and symptoms. *Brain* 1998;121:687–697. [PubMed: 9577394]
10. Stevenson V, et al. Spinal cord atrophy and disability in MS: a longitudinal study. *Neurology* 1998;51:234–238. [PubMed: 9674808]
11. Giovannoni G, et al. Soluble E-selectin in multiple sclerosis: raised concentrations in patients with primary progressive disease. *J Neurol Neurosurg Psychiatry* 1996;60:20–26. [PubMed: 8558145]
12. McDonnell G, et al. Raised CSf levels of soluble adhesion molecules across the clinical spectrum of multiple sclerosis. *J Neuroimmunol* 1998;85:186–192. [PubMed: 9630167]
13. Olerup O, et al. Primary chronic progressive and relapsing remitting multiple sclerosis: two immunogenetically distinct disease entities. *Proc Natl Acad Sci USA* 1989;86:7113–7117. [PubMed: 2571150]
14. Hillert J, et al. An immunogenetic heterogeneity in multiple sclerosis. *J Neurol Neurosurg Psychiatry* 1992;55:887–890. [PubMed: 1359021]
15. Weinshender B. The natural history of multiple sclerosis. *Neurol Clin* 1995;13:119–146. [PubMed: 7739500]
16. Revesz T, et al. A comparison of the pathology of primary and secondary progressive multiple sclerosis. *Brain* 1994;117:759–765. [PubMed: 7922463]
17. Urenjak J, Williams SR, Gadian DG, Noble M. Specific expression of N-acetylaspartate in neurons, oligodendrocyte-type-2 astrocyte progenitors, and immature oligodendrocytes in vitro. *J Neurochem* 1992;59:55–61. [PubMed: 1613513]
18. Chang L, et al. Proton spectroscopy in myotonic dystrophy: correlations with CTG repeats [see comments]. *Arch Neurol* 1998;55:305–311. [PubMed: 9520004]
19. Urenjak J, Williams SR, Gadian DG, Noble M. Proton nuclear magnetic resonance spectroscopy unambiguously identifies different neural cell types. *J Neurosci* 1993;13:981–989. [PubMed: 8441018]
20. Jagannathan NR, Desai NG, Raghunathan P. Brain metabolite changes in alcoholism: An in vivo proton magnetic resonance spectroscopy (MRS) study. *Magn Reson Imaging* 1996;14:553–557. [PubMed: 8843367]
21. Pan JW, et al. Evaluation of multiple sclerosis by 1H spectroscopic imaging at 4.1 T. *Magn Reson Med* 1996;36:72–77. [PubMed: 8795023]
22. Matthews PM, et al. Assessment of lesion pathology in multiple sclerosis using quantitative MRI morphometry and magnetic resonance spectroscopy. *Brain* 1996;119:715–722. [PubMed: 8673485]
23. Narayanan S, et al. Imaging of axonal damage in multiple sclerosis: spatial distribution of magnetic resonance imaging lesions. *Ann Neurol* 1997;41:385–391. [PubMed: 9066360]
24. Sarchielli P, et al. Absolute quantification of brain metabolites by proton magnetic resonance spectroscopy in normal appearing white matter of multiple sclerosis. *Brain* 1999;122:513–521. [PubMed: 10094259]
25. Husted CA, et al. Biochemical alterations in multiple sclerosis lesions and normal appearing white matter detected by in vivo 31P and 1H spectroscopic imaging. *Ann Neurol* 1994;36:157–165. [PubMed: 8053651]
26. Rooney WD, et al. 1H MRSI of normal appearing white matter in multiple sclerosis. *Multiple Sclerosis* 1997;3:231–237. [PubMed: 9372505]



27. Davie CA, et al. 1H magnetic resonance spectroscopy of chronic cerebral white matter lesions and normal appearing white matter in multiple sclerosis. *J Neurol Neurosurg Psychiatry* 1997;63:736–742. [PubMed: 9416807]
28. Pan JW, Whitaker JN. Quantitation of 1H metabolites in subtypes of multiple sclerosis by spectroscopic imaging at 4.1 T. *Int Soc Magn Reson Med*. 1998(Abstract)
29. Presciutti O, et al. 1H MRS study of normal appearing white matter in multiple sclerosis patients. *Int Soc Magn Reson Med*. 1998(Abstract)
30. Schumacher GA, Beebe G, Kibler RE. Problems of experimental trials of therapy in multiple sclerosis: report by the panel on evaluation of experimental trials of therapy in multiple sclerosis. *Ann NY Acad Sci* 1965;122:552–568. [PubMed: 14313512]
31. Lublin F, Reingold S. Defining the clinical course of multiple sclerosis: results of an international survey. *Neurology* 1996;46:907–911. [PubMed: 8780061]
32. Andersson P, Waubant E, Gee L, Goodkin DE. Multiple sclerosis progressive from onset: clinical characteristics and progression of disability. *Arch Neurol*. 1999(In Press)
33. Maudsley AA, Matson GB, Hugg JW, Weiner MW. Reduced phase encoding in spectroscopic imaging. *Magn Reson Med* 1994;31:645–651. [PubMed: 8057817]
34. Maudsley AA, Lin E, Weiner MW. Spectroscopic imaging display and analysis. *Magn Reson Imaging* 1992;10:471–485. [PubMed: 1406098]
35. Soher BJ, Young K, Govindaraju V, Maudsley AA. Automated spectral analysis III: Application to in vivo proton MR spectroscopy and spectroscopic imaging. *Magn Res Med* 1998;40:822–831.
36. Pan JW, Twieg DB, Hetherington HP. Quantitative spectroscopic imaging of the human brain. *Magn Reson Med* 1998;40:363–369. [PubMed: 9727938]
37. Benjamini Y, Hochberg Y. Controlling the false discovery rate: a practical and powerful approach to multiple testing. *J R Statist Soc B* 1995;57:289–300.
38. McDonnell G, Hawkins SA. Clinical study of primary progressive multiple sclerosis in Northern Ireland, UK. *J Neurol Neurosurg Psychiatry* 1998;64:451–454. [PubMed: 9576534]
39. De Stefano N, et al. Axonal damage correlates with disability in patients with relapsing-remitting multiple sclerosis. Results of a longitudinal magnetic resonance spectroscopy study. *Brain* 1998;121:1469–1477. [PubMed: 9712009]
40. Fu L, et al. Imaging axonal damage of normal-appearing white matter in multiple sclerosis. *Brain* 1998;121:103–113. [PubMed: 9549491]

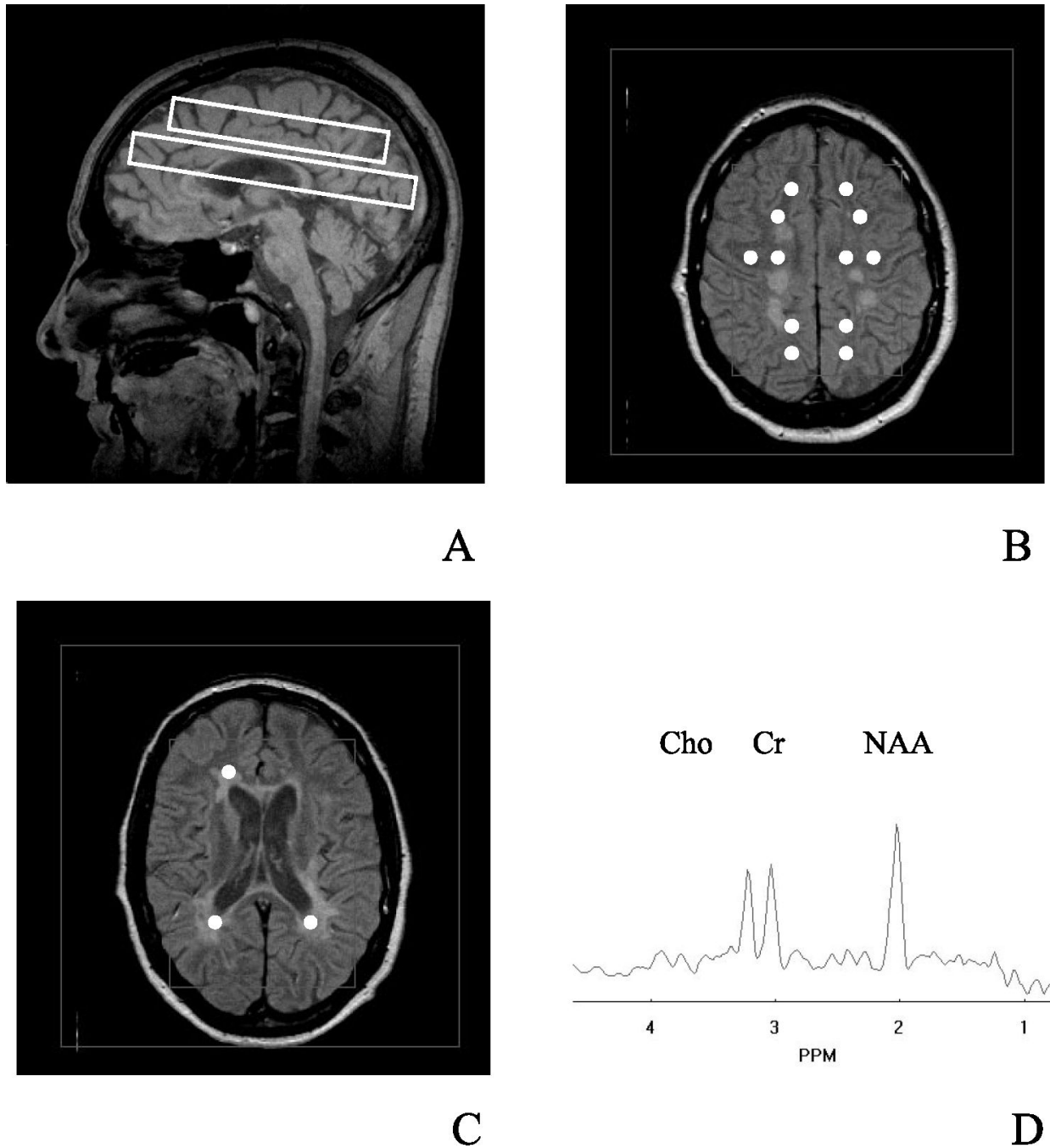


**Figure 1.** Scout sagittal MRI of PPMS patient showing position of the <sup>1</sup>H MRSI VOI by inner rectangles and FOV by outer rectangle (A). <sup>1</sup>H MRSI VOIs were angulated along AC-PC line. The axial MRI from the center of the supra-ventricular <sup>1</sup>H MRSI VOI is displayed in (B) and of the periventricular VOI is displayed in (C) as inner rectangles. The <sup>1</sup>H MRSI FOV is indicated by the outer rectangles in (B and C). Typical <sup>1</sup>H MRSI voxel positions were selected as indicated by white circles; NAWM from (B) and lesions from (C). A representative <sup>1</sup>H MRSI spectrum from NAWM is shown in (D)

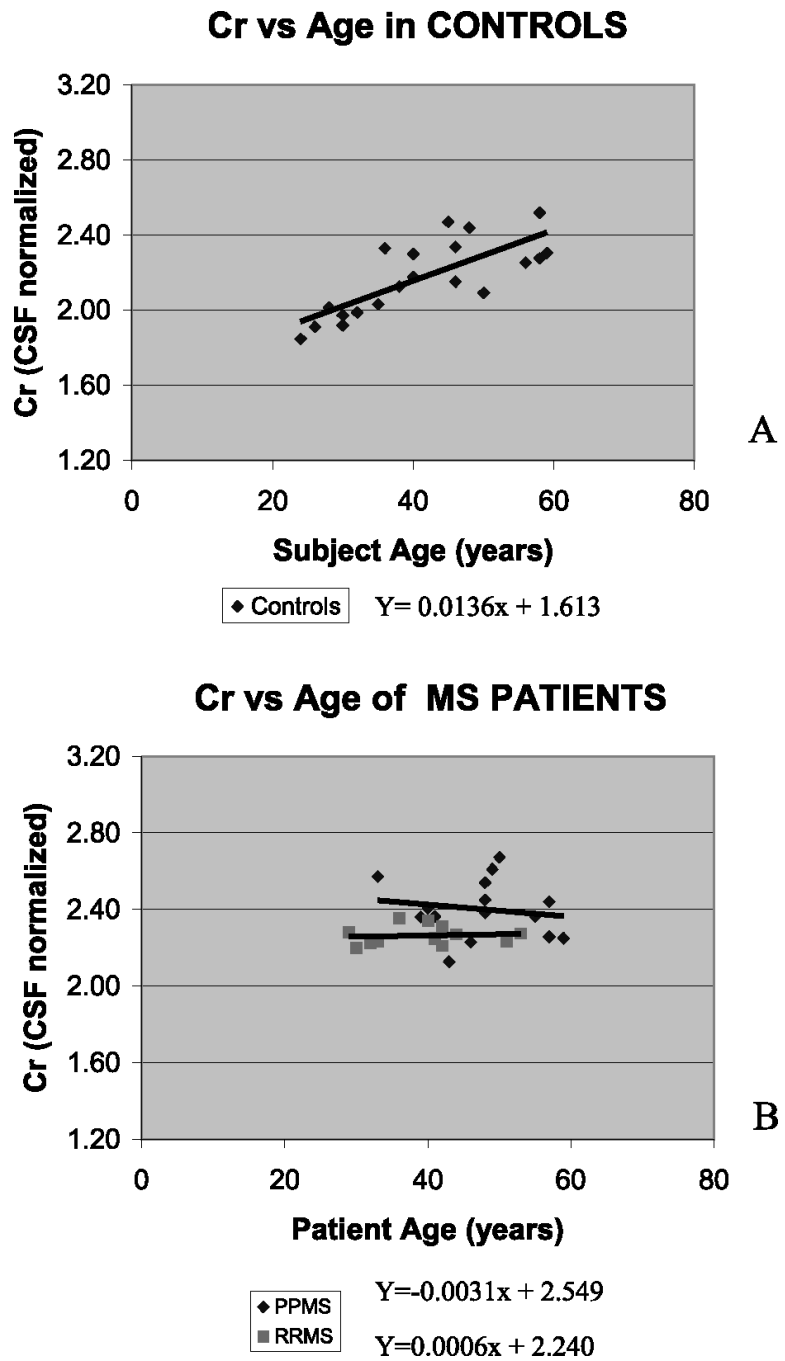


**Figure 2.** Regression analysis plot of Cr versus age in NAWM of controls (A) and Cr versus age in NAWM of both MS patient groups (B)

Table 1

Ratios and CSF normalized values of metabolites in NAWM of MS patients and healthy controls. Values are reported as mean±standard deviation

Subjects	n	NAA/Cr	NAA/Cho	NAA	Cr	Cho
PPMS	15	1.90±0.11	1.86±0.30	4.55±0.35	2.40±0.15	2.53±0.41
RRMS	13	2.04±0.09	1.97±0.25	4.59±0.17	2.26±0.05	2.39±0.32
Controls	20	2.22±0.19	1.95±0.22	4.77±0.28	2.17±0.20	2.49±0.23

<i>P</i> values <sup>1</sup>	NAA/Cr	NAA/Cho	NAA	Cr	Cho
PPMS/RRMS	0.031	0.313	0.585	0.038	0.329
PPMS/Controls	0.027 <sup>2</sup>	0.302	0.047 <sup>&lt;</sup>	0.035 <sup>&gt;</sup>	0.642
RRMS/Controls	0.027 <sup>2</sup>	0.833	0.047	0.044 <sup>2</sup>	0.370

<sup>1</sup> Corrected for multiple comparisons

<sup>2</sup> Controlled for age;

< One-sided comparison due to a priori hypotheses

> One-sided comparison due to a priori hypotheses

**Table 2**

Ratios and CSF normalized values of metabolites in lesions of MS patients and equivalent white matter regions in controls. Values are reported as mean±standard deviation

Subjects	n	NAA/Cr	NAA/Cho	NAA	Cr	Cho
PPMS	12	1.73±0.31	1.48±0.31	3.97±0.47	2.35±0.23	2.86±0.59
RRMS	10	1.87±0.39	1.56±0.41	3.74±0.64	2.03±0.22	2.52±0.39
Controls	15	2.14±0.18	1.81±0.22	4.42±0.29	2.11±0.19	2.52±0.32

<i>P</i> values <sup>1</sup>	NAA/Cr	NAA/Cho	NAA	Cr	Cho
PPMS/RRMS	0.359	0.610	0.497	0.044	0.153
PPMS/Controls	0.027 <sup>2</sup>	0.046	0.036 <sup>&lt;</sup>	0.041 <sup>&lt;</sup>	0.087
RRMS/Controls	0.048 <sup>2</sup>	0.080	0.031	0.647 <sup>2</sup>	0.983

<sup>1</sup> Corrected for multiple comparisons

<sup>2</sup> Controlled for age

< One-sided comparison due to a priori hypotheses

> One-sided comparison due to a priori hypotheses